Supporting information for

Single molecule magnet behavior and luminescence of {Ln_4} and {LnZn} complexes

Guo Peng,[a]* Qi Yang,[a] Yue Chen,[a] Xiang-Tao Dong, [a] Zaichao Zhang[b] and Xiao-Ming Ren[a]*

[a]State Key Laboratory of Materials-Oriented Chemical Engineering, School of Chemistry and Molecular Engineering, Nanjing Tech University, Nanjing 211816, P. R. China

E-mail: guopeng@njtech.edu.cn, xmren@njtech.edu.cn

[b] Jiangsu Key Laboratory for the Chemistry of Low-Dimensional Materials, School of Chemistry and Chemical Engineering, Huaiyin Normal University, Huai'an 223300, China

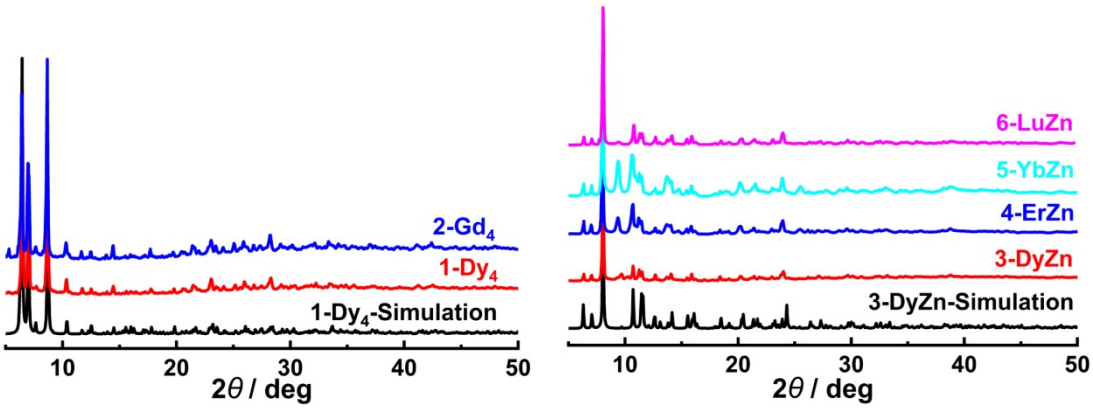

(a) (b)

Fig. S1 Measured and simulated PXRD patterns of complexes **1**-**6**.

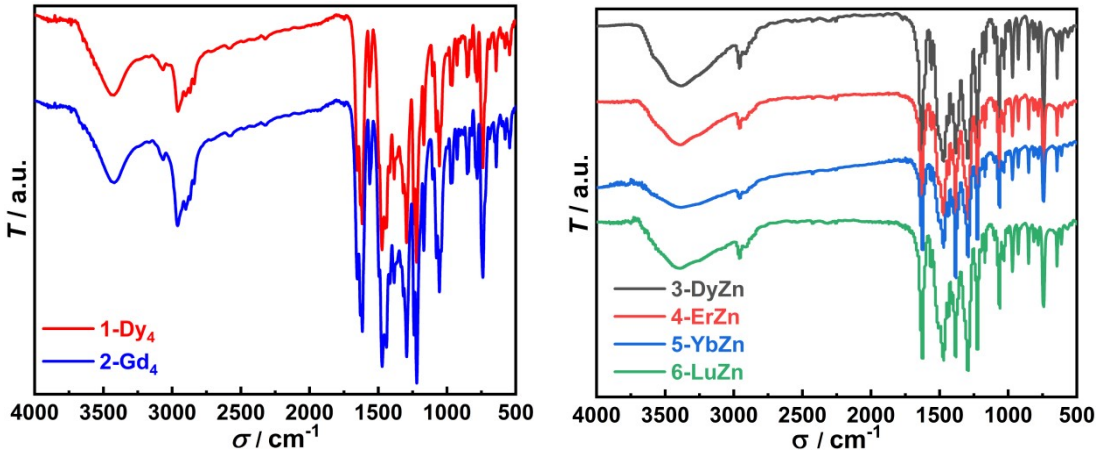

Fig. S2 IR spectra of complexes **1**-**6**.

Table S1. Crystallographic data and structure refinement for ligand and complexes **1**-**5**.

	Ligand	1-Dy_4	2-Gd_4
Formula	$C_{21}H_{26}N_2O_4$	$C_{90}H_{119}Dy_4N_{15}O_{35}$	$C_{92}H_{122}Gd_4N_{16}O_{35}$
M_r (g mol^{-1})	370.44	2620.99	2641.04
Crystal system	Triclinic	Monoclinic	Monoclinic
Space group	*P-1*	*C*2/c	*C*2/c
T (K)	173(2)	173(2)	173(2)
a (Å)	13.0277(4)	30.2530(9)	30.398(4)
b (Å)	13.5623(4)	17.0358(4)	17.011(2)
c (Å)	13.8395(5)	24.1031(6)	24.192(5)
α (º)	108.0940(10)	90	90
β (º)	107.9440(10)	123.388(3)	123.5970(10)
γ (º)	110.0100(10)	90	90
V (Å^3)	1934.75(11)	10372.2(6)	10419(3)
Z	4	4	4
D_c (g cm^{-3})	1.272	1.678	1.684
μ (mm^{-1})	0.088	2.916	2.584
F(000)	792	4644	4612
Reflns collected	16380	46944	22275
Unique reflns	7053	11209	9393
R_{int}	0.0378	0.0298	0.0830
GOF	0.989	1.059	1.033

R_1(I > 2σ)	0.0417	0.0220	0.0488
wR_2 (all data)	0.1119	0.0614	0.0973
Max. diff. peak / hole (e Å^{-3})	0.168/-0.215	1.478/-0.852	0.981/-0.950
	3-DyZn	4-ErZn	5-YbZn
Formula	$C_{25}H_{32}N_7O_{14}ZnDy$	$C_{25}H_{32}N_7O_{14}ZnEr$	$C_{25}H_{32}N_7O_{14}ZnYb$
M_r (g mol^{-1})	882.44	887.20	892.98
Crystal system	triclinic	triclinic	triclinic
Space group	*P*-1	*P*-1	*P*-1
T (K)	173(2)	173(2)	173(2)
a (Å)	9.1667(4)	9.1607(4)	9.1368(5)
b (Å)	13.0847(6)	13.0748(7)	13.0737(8)
c (Å)	14.5952(6)	14.5902(7)	14.5753(8)
α (º)	73.713(2)	73.561(2)	73.361(2)
β (º)	88.479(2)	88.3920(10)	88.269(2)
γ (º)	84.283(2)	84.147(2)	84.129(2)
V (Å^3)	1671.99(13)	1667.36(14)	1659.39(16)
Z	2	2	2
D_c (g cm^{-3})	1.753	1.767	1.787
μ (mm^{-1})	3.010	3.294	3.599
F(000)	878	882	886
Reflns collected	13497	14035	13843
Unique reflns	6013	6056	6013
R_{int}	0.0389	0.0445	0.0376
GOF	1.064	1.059	1.050
R_1(I > 2σ)	0.0305	0.0345	0.0307
wR_2 (all data)	0.0539	0.0621	0.0533
Max. diff. peak / hole (e Å^{-3})	0.669/-0.578	1.069/-0.783	1.111/-0.920

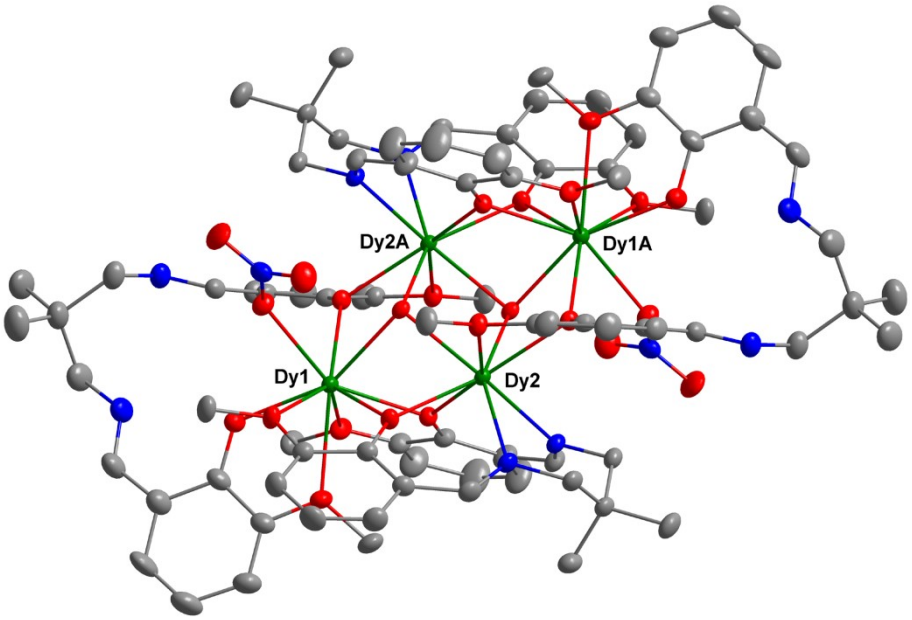

(a)

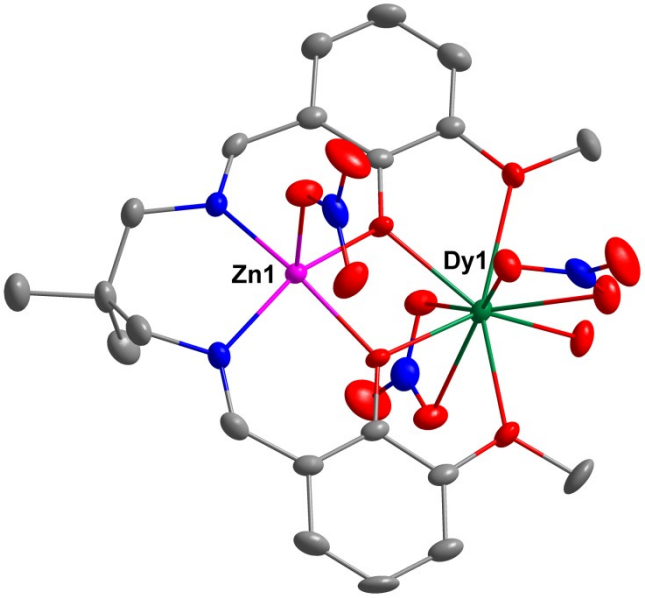

(b)

Fig. S3 ORTEP views of complexes **1** (a) and **3** (b) with displacement ellipsoids drawn at the 50% probability level. Symmetry codes: A 1.5-x, 0.5-y, 1-z.

Table S2. Continuous shape measures (CShM) for complexes **1-Dy_4** and **2-Gd_4**.

	Dy1	Gd1		Dy2	Gd2
EP-9	35.756	35.766	OP-8	31.365	31.689
OPY-9	22.105	22.247	HPY-8	20.569	20.377
HBPY-9	17.117	17.027	HBPY-8	14.899	14.629
JTC-9	16.389	16.501	CU-8	8.479	8.296
JCCU-9	10.021	9.873	SAPR-8	**1.292**	**1.341**
CCU-9	8.640	8.461	TDD-8	2.271	2.316
JCSAPR-9	1.862	1.944	JGBF-8	15.349	15.383
CSAPR-9	**1.206**	**1.251**	JETBPY-8	26.478	26.492
JTCTPR-9	3.561	3.585	JBTPR-8	3.471	3.595
TCTPR-9	1.517	1.531	BTPR-8	2.986	3.094
JTDIC-9	12.655	12.708	JSD-8	5.443	5.549
HH-9	10.993	10.718	TT-8	9.192	9.001
MFF-9	**1.225**	**1.261**	ETBPY-8	22.465	22.542

EP-9=Enneagon, OPY-9=Octagonal pyramid, HBPY-9=Heptagonal bipyramid, HBPY-9=Heptagonal bipyramid, JCCU-9=Capped cube J8, CCU-9=Spherical-relaxed capped cube, JCSAPR-9=Capped square antiprism J10, CSAPR-9=Spherical capped square antiprism, JTCTPR-9=Tricapped trigonal prism J51, TCTPR-9=Spherical tricapped trigonal prism, JTDIC-9=Tridiminished icosahedron J63, HH-9=Hula-hoop, MFF-9=Muffin; OP-8=Octagon, HPY-8=Heptagonal pyramid, HBPY-8=Hexagonal bipyramid, CU-8=Cube, SAPR-8=Square antiprism, TDD-8=Triangular dodecahedron, JGBF-8=Johnson gyrobifastigium J26, JETBPY-8=Johnson elongated triangular bipyramid J14, JBTPR-8=Biaugmented trigonal prism J50, BTPR-8=Biaugmented trigonal prism, JSD-8=Snub diphenoid J84, TT-8=Triakis tetrahedron, ETBPY-8=Elongated trigonal bipyramid

Table S3. Continuous shape measures (CShM) for complexes **3-DyZn, 4-ErZn** and **5-YbZn**.

	Zn			Ln			
	3-DyZn	4-ErZn	5-YbZn		3-DyZn	4-ErZn	5-YbZn
PP-5	26.834	26.853	26.817	EP-9	36.049	36.072	36.055
vOC-5	3.027	3.041	3.088	OPY-9	21.943	22.047	22.029

TBPY-5	5.202	5.265	5.328	HBPY-9	16.200	16.354	16.462
SPY-5	**1.636**	**1.634**	**1.629**	JTC-9	14.471	14.706	14.876
JTBPY-5	7.926	8.039	8.088	JCCU-9	10.438	10.522	10.715
				CCU-9	8.458	8.551	8.716
				JCSAPR-9	2.968	2.828	2.724
				CSAPR-9	**1.776**	**1.634**	**1.530**
				JTCTPR-9	4.242	4.199	4.151
				TCTPR-9	2.530	2.457	2.418
				JTDIC-9	10.192	10.381	10.560
				HH-9	10.876	11.034	11.026
				MFF-9	**1.923**	**1.800**	**1.722**

PP-5 = Pentagon, vOC-5 = Vacant octahedron, TBPY-5 = Trigonal bipyramid, SPY-5 = Spherical square pyramid, JTBPY-5 = Johnson trigonal bipyramid J12; EP-9=Enneagon, OPY-9=Octagonal pyramid, HBPY-9=Heptagonal bipyramid, HBPY-9=Heptagonal bipyramid, JCCU-9=Capped cube J8, CCU-9=Spherical-relaxed capped cube, JCSAPR-9=Capped square antiprism J10, CSAPR-9=Spherical capped square antiprism, JTCTPR-9=Tricapped trigonal prism J51, TCTPR-9=Spherical tricapped trigonal prism, JTDIC-9=Tridiminished icosahedron J63, HH-9=Hula-hoop, MFF-9=Muffin

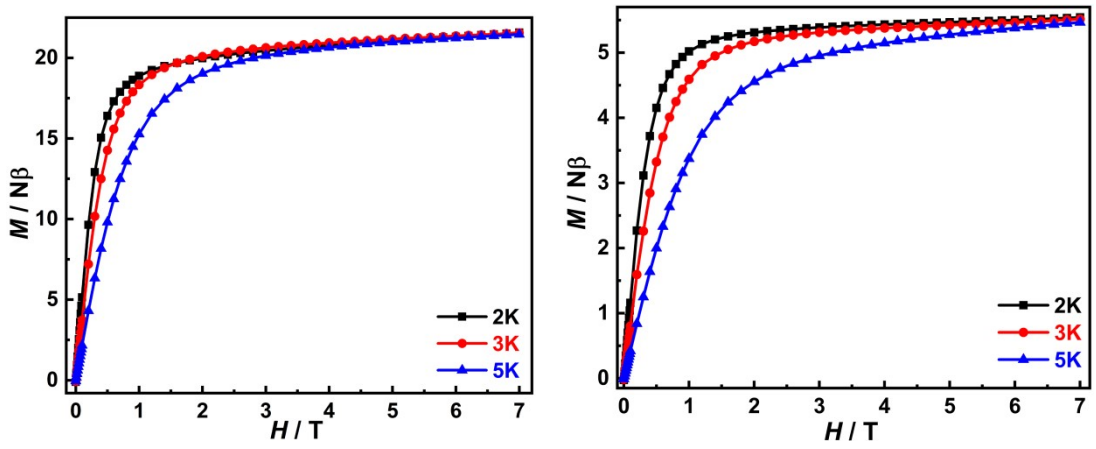

(a) (b)

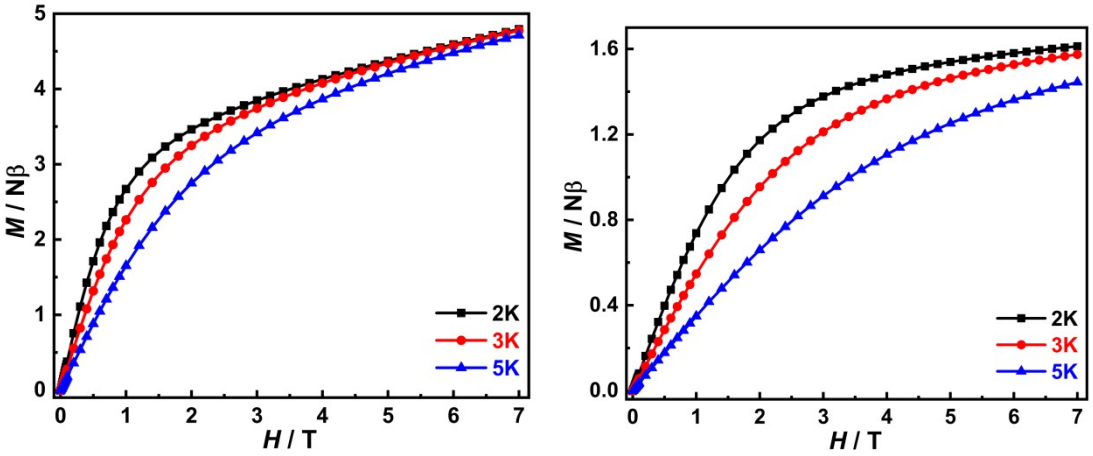

Fig. S4 *M* vs. *H* curves for **1** (a) and **3-5** (b-d).

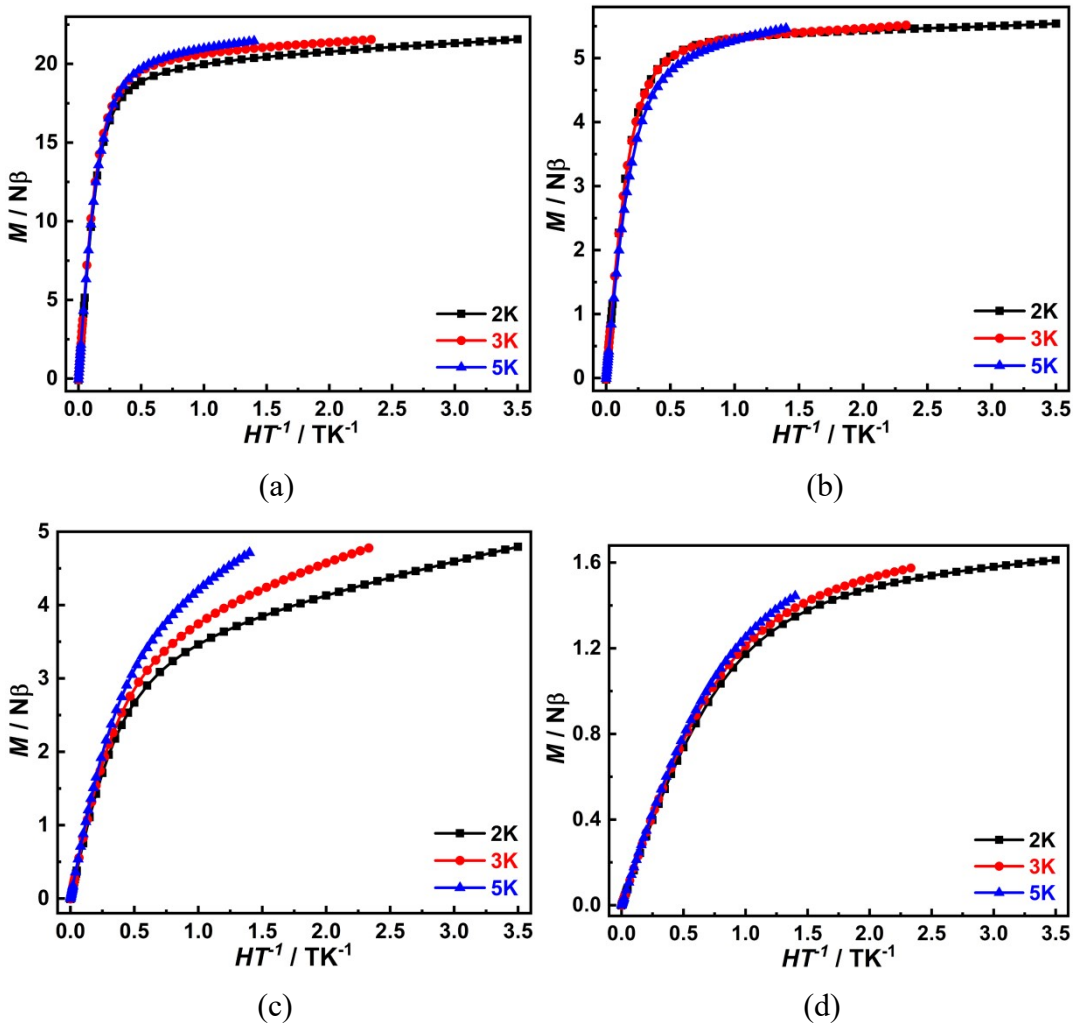

Fig. S5 *M* vs. HT^{-1} curves for **1** (a) and **3-5** (b-d).

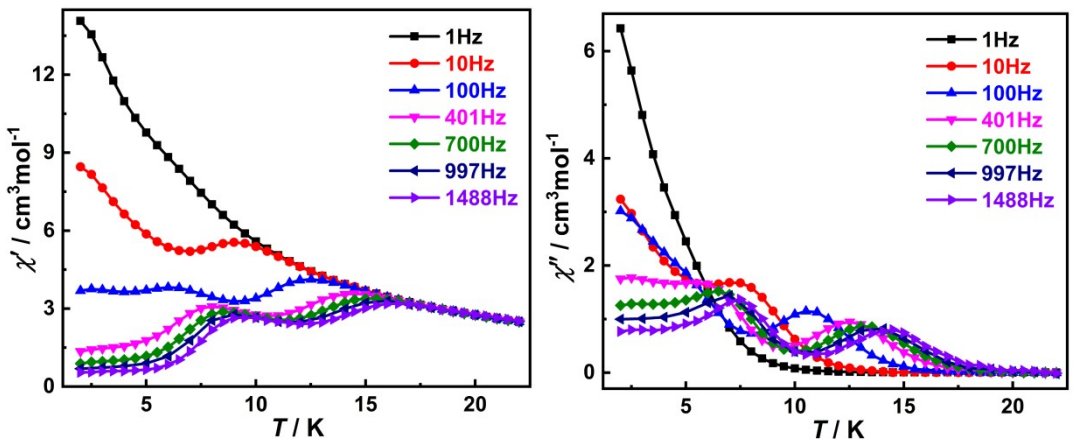

(a) (b)

Fig. S6 Temperature dependence of in-phase (a) and out-of-phase (b) ac susceptibility under a zero dc field for **1**.

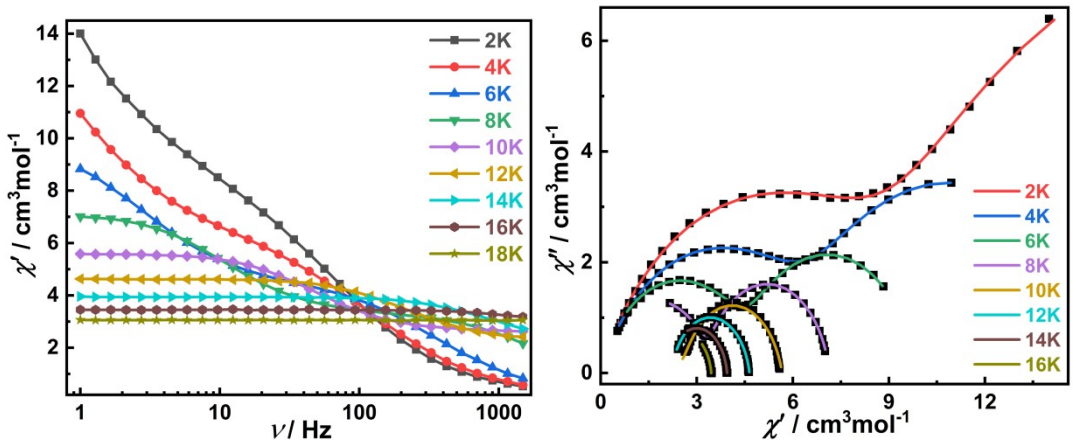

(a) (b)

Fig. S7 Frequency dependence of in-phase (a) ac susceptibility under a zero dc field and Cole-Cole plots (b) for **1**.

Table S4. Cole-Cole parameters of **1** at a zero dc field

T / K	χ_S / cm^3·mol^{-1}	$\Delta\chi_1$ / cm^3·mol^{-1}	τ_1 / s	α_1	$\Delta\chi_2$ / cm^3·mol^{-1}	τ_2 / s	α_2	R
2	1.38E-08	9.08E+00	2.53E-03	2.96E-01	2.18E+01	4.50E-01	2.43E-01	1.27E-01
4	2.23E-08	6.60E+00	1.37E-03	2.94E-01	9.19E+00	1.69E-01	2.19E-01	8.43E-03
6	6.30E-08	4.60E+00	4.32E-04	2.34E-01	5.27E+00	5.54E-02	1.62E-01	9.28E-03
8	2.99E-07	3.36E+00	6.82E-05	1.76E-01	3.78E+00	1.43E-02	1.18E-01	7.07E-03
10	4.63E-14	2.73E+00	8.03E-08	6.73E-01	2.95E+00	3.22E-03	1.39E-01	1.04E-01
12	4.00E-15	2.21E+00	3.19E-07	8.86E-07	2.43E+00	6.91E-04	1.22E-01	1.38E-02
14	3.80E-22	2.11E+00	1.31E-06	3.57E-06	1.84E+00	1.69E-04	9.20E-02	3.86E-03
16	2.83E-30	2.11E+00	3.03E-06	6.46E-06	1.34E+00	4.69E-05	9.22E-02	3.20E-03

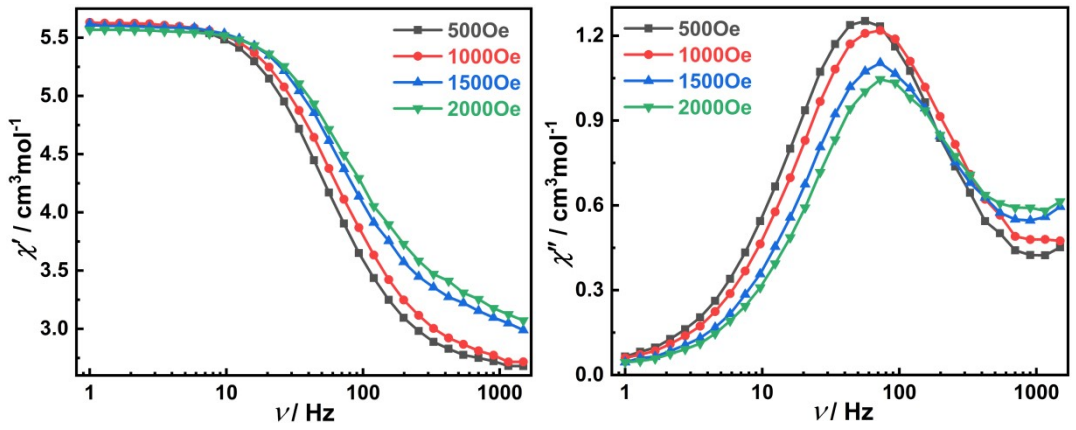

(a) (b)

Fig. S8 Frequency dependence of in-phase (a) and out-of-phase (b) ac susceptibility under various dc fields at 10 K for **1**.

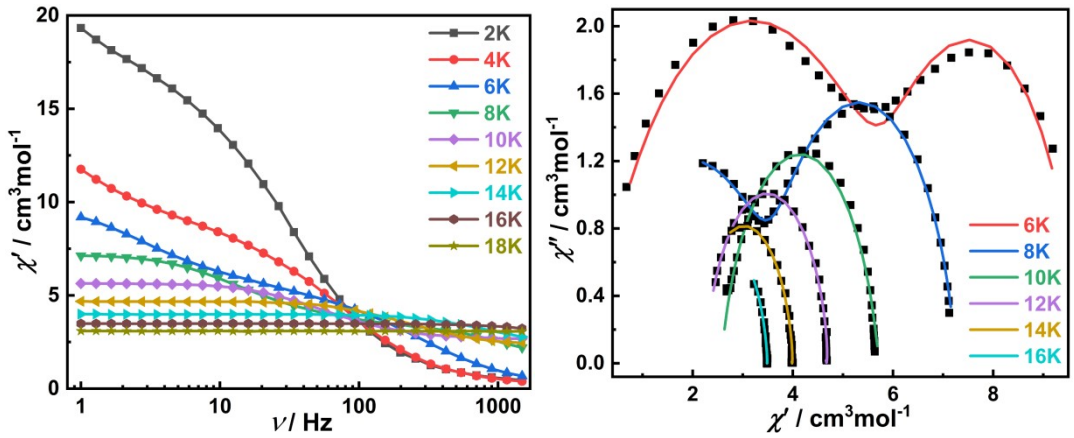

(a) (b)

Fig. S9 Frequency dependence of in-phase (a) ac susceptibility under a 500Oe dc field and Cole-Cole plots (b) for **1**.

Table S5. Cole-Cole parameters of **1** at a 500Oe dc field.

T / K	χ_S / cm^3·mol^{-1}	$\Delta\chi_1$ / cm^3·mol^{-1}	τ_1 / s	α_1	$\Delta\chi_2$ / cm^3·mol^{-1}	τ_2 / s	α_2	R
6	4.04E-14	6.07 E+00	7.52E-04	2.68E-01	3.60 E+00	5.15E-02	4.85E-02	2.19E -01
8	1.09E-13	3.68 E+00	7.29E-05	2.84E-01	3.58 E+00	1.08E-02	1.30E-01	3.18E -02
10	3.13E-13	4.26 E+00	3.54E-21	9.89E-01	3.04 E+00	2.60E-03	1.38E-01	1.79E -01
12	4.43E-13	6.82 E+00	1.05E-21	1.02E+00	2.67 E+00	6.76E-04	1.51E-01	1.32E -02
14	2.05E-12	4.72 E+00	3.98E-21	1.01E+00	2.03 E+00	1.58E-04	1.26E-01	4.99E -03
16	4.96E-12	3.75 E+00	9.01E-21	1.00E+00	1.71 E+00	3.54E-05	1.11E-01	1.92E -03

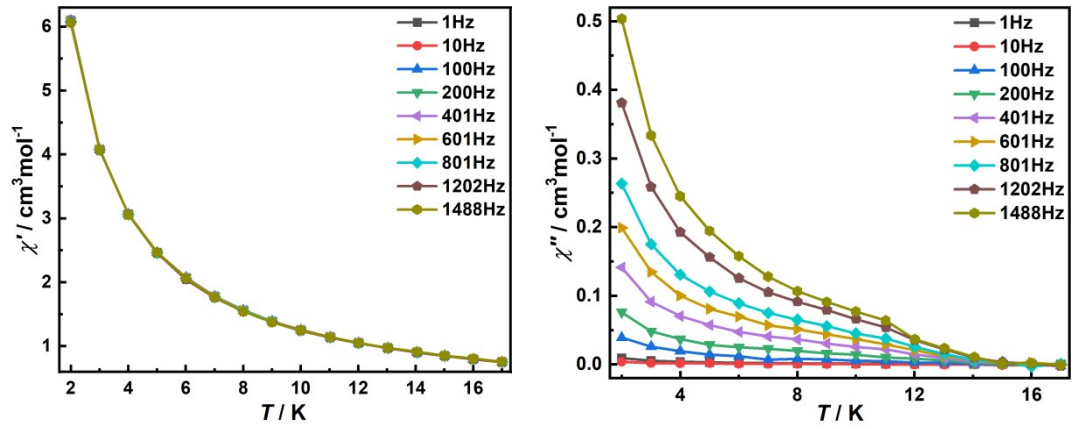

(a) (b)

Fig. S10 Temperature dependence of in-phase (a) and out-of-phase (b) ac susceptibility at a zero dc field for **3**.

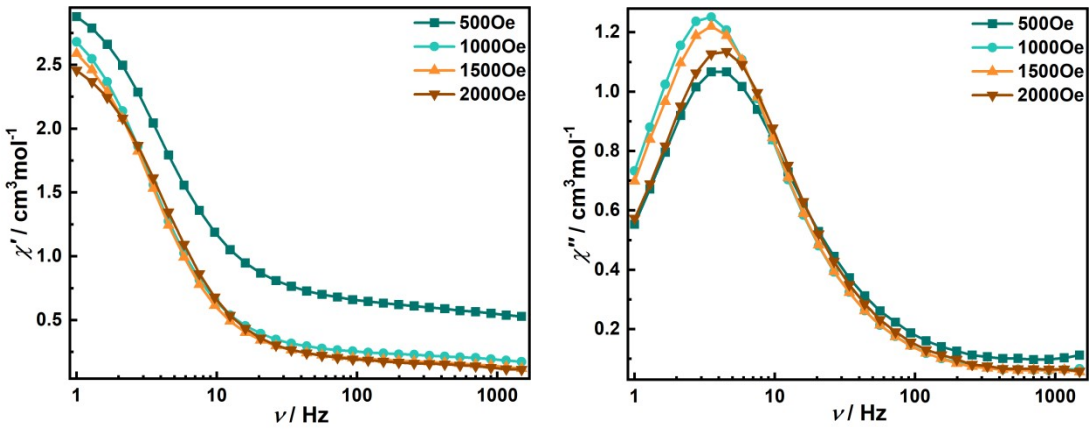

(a) (b)

Fig. S11 Frequency dependence of in-phase (a) and out-of-phase (b) ac susceptibility under various dc fields at 4 K for **3**.

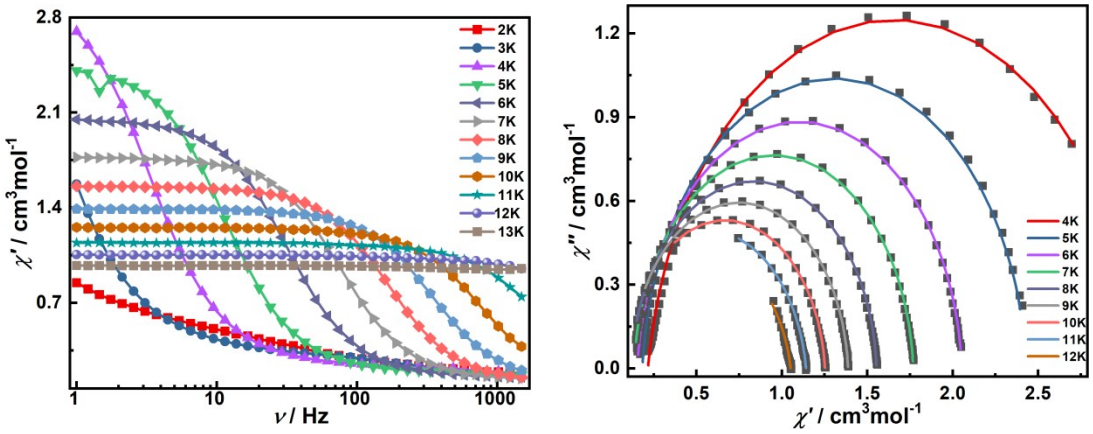

(a) (b)

Fig. S12 Frequency dependence of in-phase (a) ac susceptibility under a 1000Oe dc field and Cole-Cole plots (b) for **3**.

Table S6. Cole-Cole parameters of **3** at a 1000Oe dc field.

T / K	χ_S / cm^{-3}mol^{-1}	χ_T / cm^{-3}mol^{-1}	τ / s	α	R
4	2.16E-1	3.10	4.86E-2	9.04E-2	3.19E-2
5	1.83E-1	2.43	1.36E-2	5.06E-2	2.55E-2
6	1.54E-1	2.05	4.96E-3	4.55E-2	2.16E-3
7	1.33E-1	1.77	2.07E-3	4.26E-2	1.23E-3
8	1.18E-1	1.55	9.57E-4	4.26E-2	6.14E-4
9	1.08E-1	1.39	4.62E-4	4.60E-2	5.87E-4
10	8.28E-2	1.25	2.04E-4	6.12E-2	7.83E-4
11	9.89E-16	1.14	7.14E-5	9.28E-2	6.75E-4
12	1.78E-15	1.04	2.33E-5	1.29E-1	1.02E-3

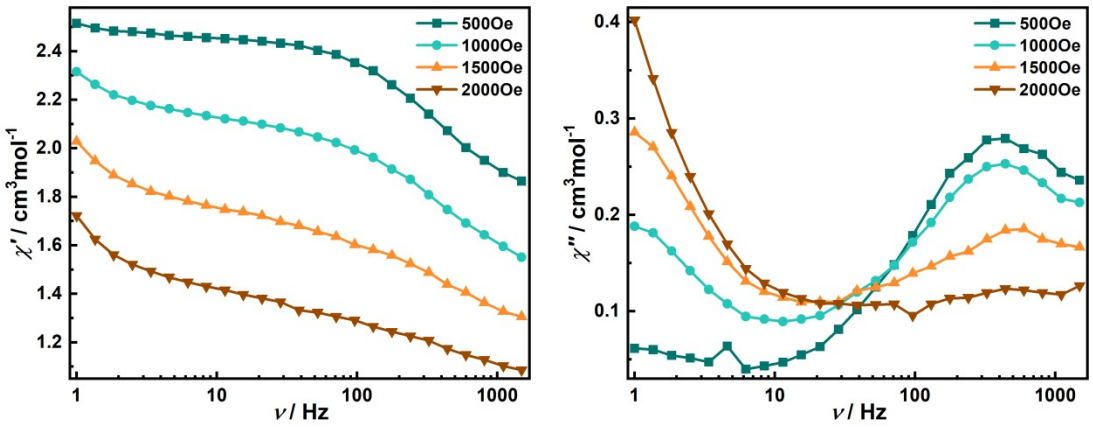

(a) (b)

Fig. S13 Frequency dependence of in-phase (a) and out-of-phase (b) ac susceptibility under various dc fields at 2 K for **4**.

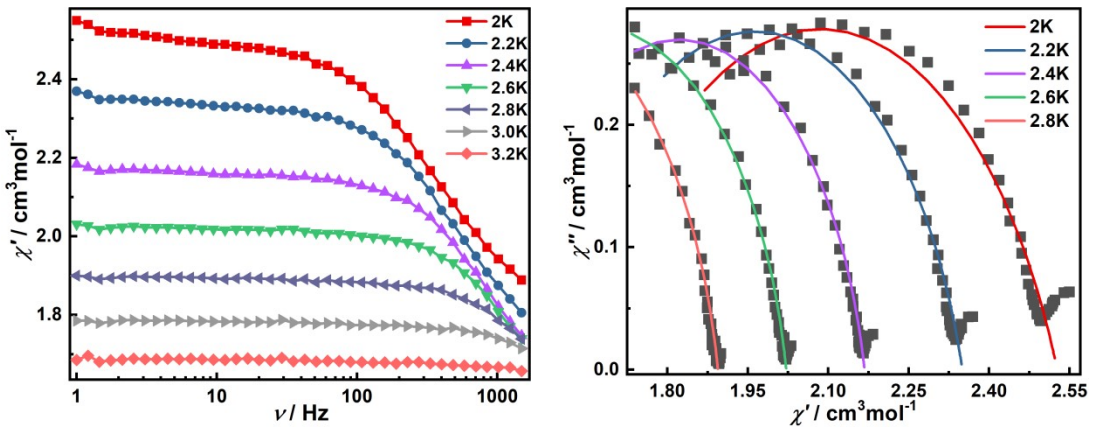

(a) (b)

Fig. S14 Frequency dependence of in-phase (a) ac susceptibility under a 500Oe dc field and Cole-Cole plots (b) for **4**.

Table S7. Cole-Cole parameters of **4** at a 500Oe dc field.

T / K	χ_S / cm^{-3}mol^{-1}	χ_T / cm^{-3}mol^{-1}	τ / s	α	R
2	1.64	2.53	3.16E-4	2.84E-1	2.04E-2
2.2	1.58	2.35	2.36E-4	2.10E-1	1.02E-2
2.4	1.48	2.16	1.54E-4	1.57E-1	4.74E-3
2.6	1.32	2.02	8.22E-5	1.45E-1	2.43E-3
2.8	1.15	1.89	4.05E-5	1.44E-1	1.31E-3

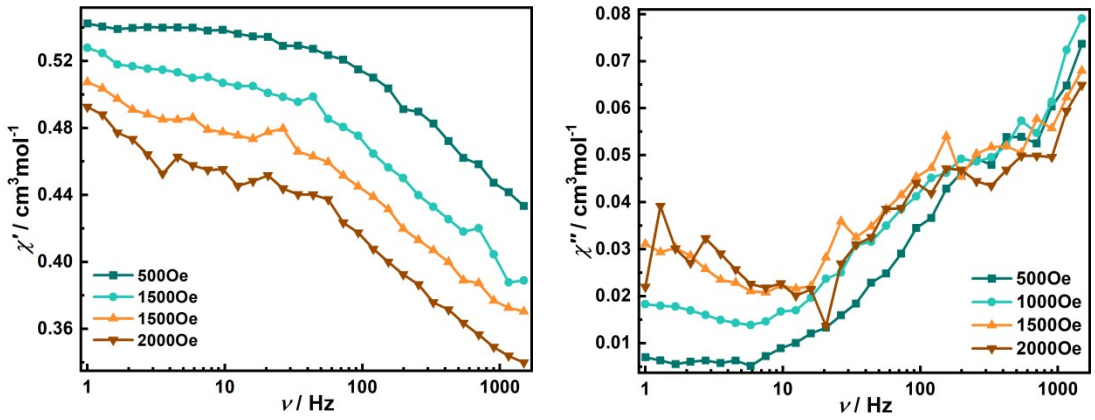

(a) (b)

Fig. S15 Frequency dependence of in-phase (a) and out-of-phase (b) ac susceptibility under various dc fields at 2 K for **5**.

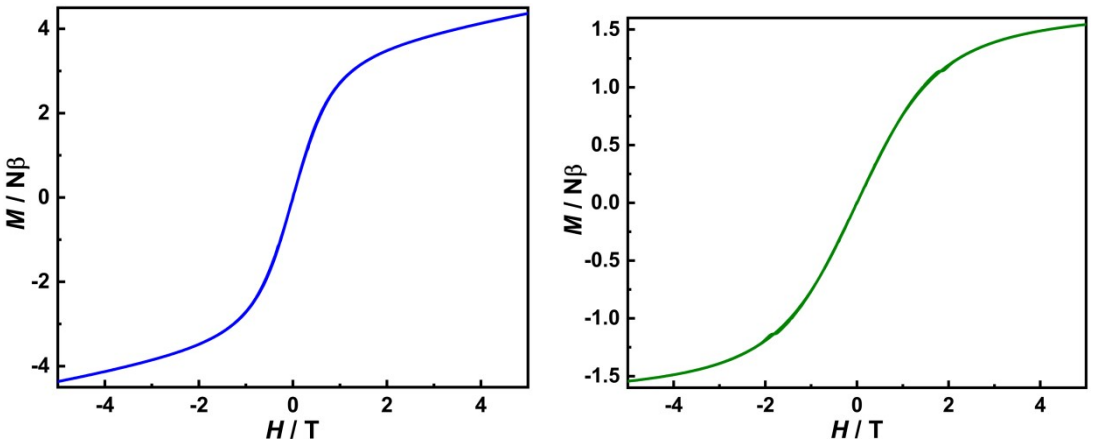

(a) (b)

Fig. S16 Field dependence of the magnetization at 2 K for **4** (a) and **5** (b).

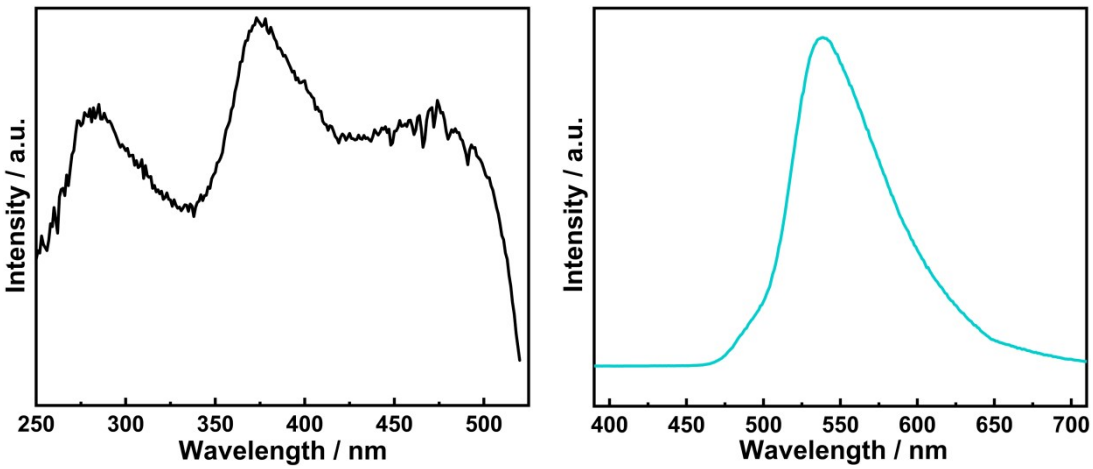

(a) (b)

Fig. S17 Excitation (a) and emission (b) spectra of the ligand.

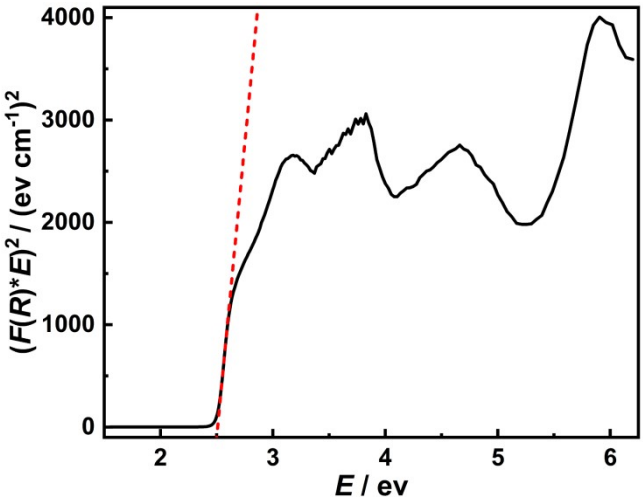

Fig. S18 Kubelka-Munk Function vs. energy curves of the ligand.

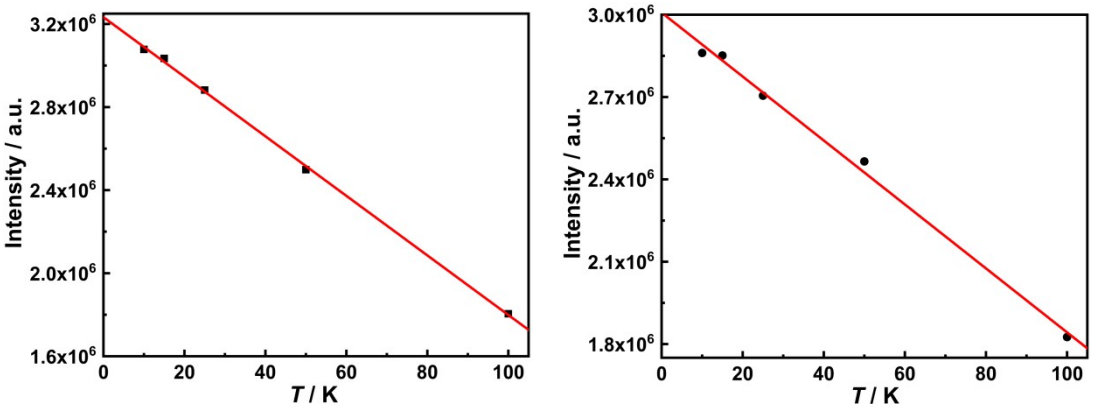

(a) (b)

Fig. S19 Emission intensity vs. temperature curves of **1** (a) and **2** (b) below 100K. The solid lines are the best linear fits to the data (R^2=0.999 for **1** and 0.994 for **2**.).

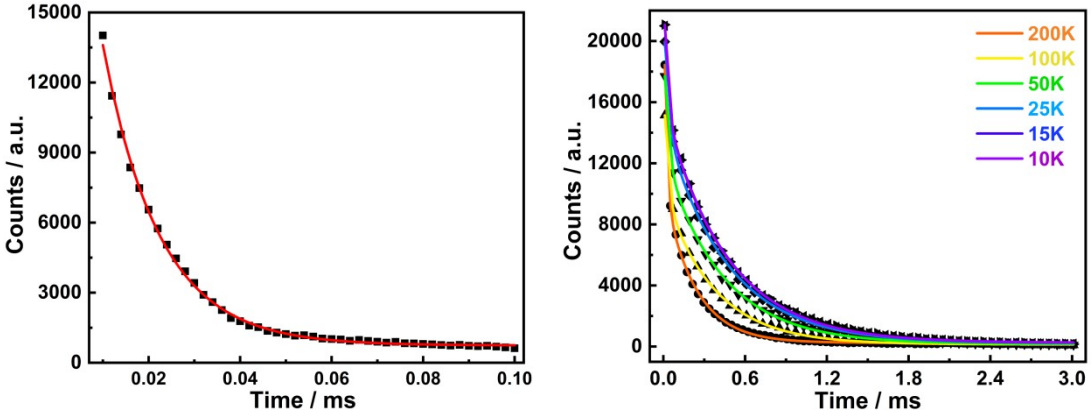

(a) (b)

Fig. S20 Lifetime decay curves for **2** at 300K (a) and below 200K (b). The solid lines are the best fit to the single (a) or double (b) exponential functions.

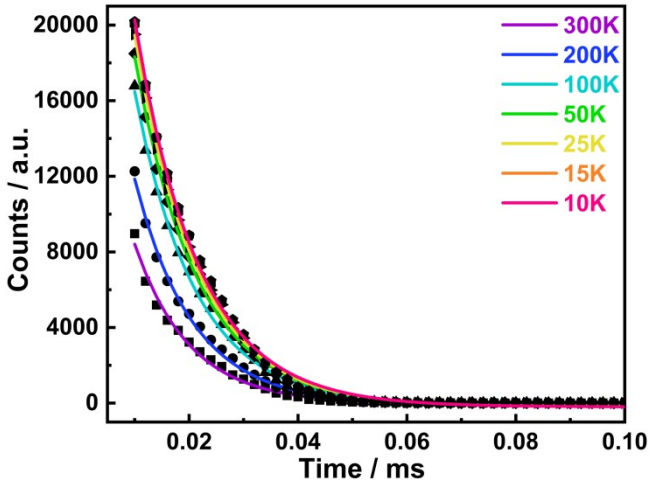

Fig. S21 Lifetime decay curves for **1** at various temperatures. The solid lines are the best fit to the double exponential functions.

Table S8. The emission lifetimes of **1** and **2** measured by using the light source with pulse width of 10μs.

	1-Dy$_4$	**2-Gd$_4$**	
T / K	τ / ms	τ_1 / ms	τ_2 / ms
300	0.010	0.012	-
200	0.011	0.018	0.23
100	0.011	0.028	0.37
50	0.011	0.030	0.42
25	0.011	0.031	0.45
15	0.012	0.027	0.46
10	0.012	0.028	0.46

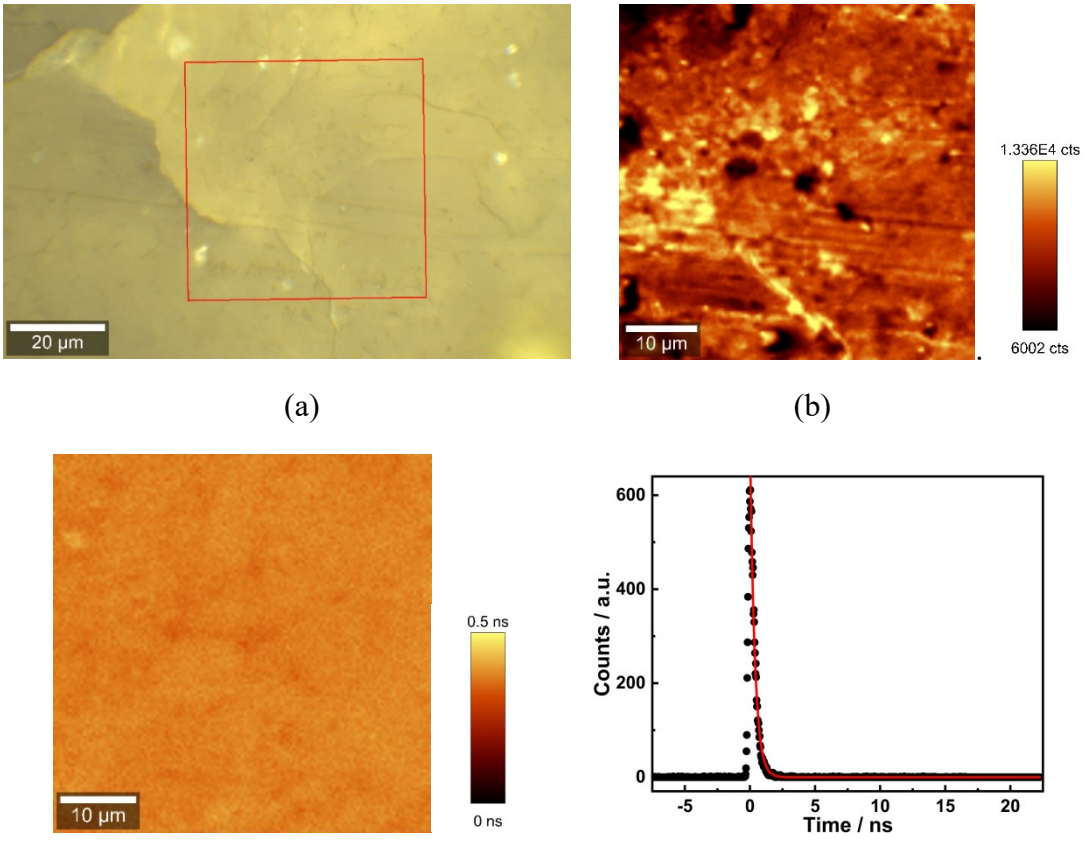

Fig. S22 (a) Optical image of the complex **1** (the scanning range is within the red frame); (b) PL intensity mapping image of complex **1**; (c) PL lifetime mapping image of complex **1**; (d) Lifetime decay curve of **1** at 300K. The red line is the best fit to the single exponential function.

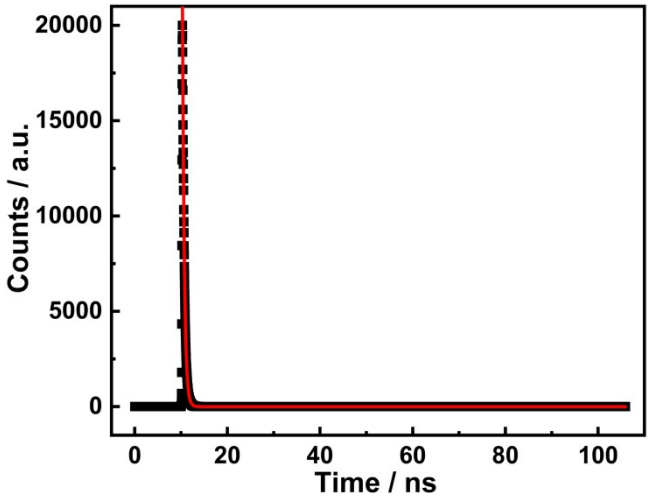

Fig. S23 Lifetime decay curve of the ligand at 300K. The red line is the best fit to the single exponential function.

Table S9. Images of **3** and **6** under day light and UV light.

Compound	Under day light	Under UV light
3-DyZn	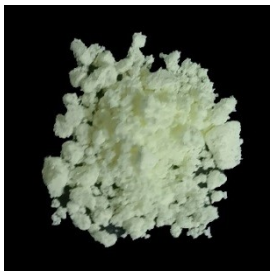	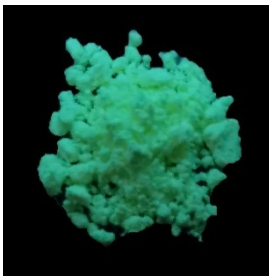
6-LuZn		

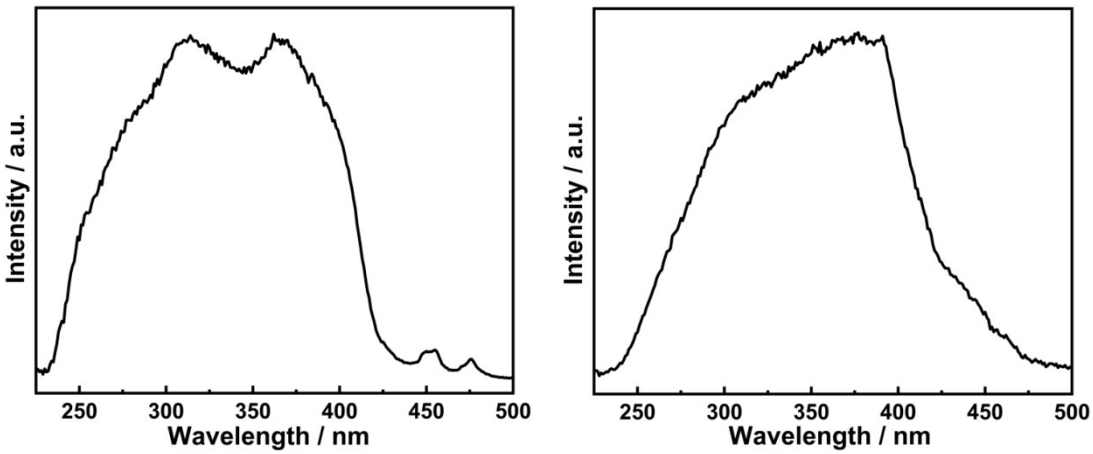

(a) (b)

Fig. S24 Excitation spectra of **3** (a) and **5** (b).

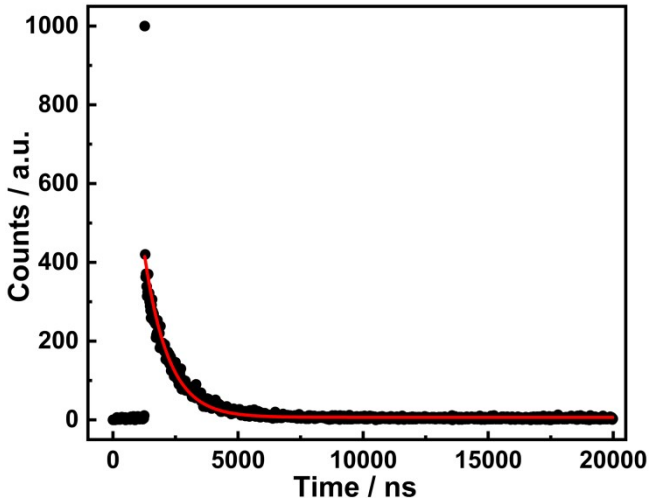

Fig. S25 Lifetime decay curve of **3** at 300K. The red line is the best fit to the single exponential function.

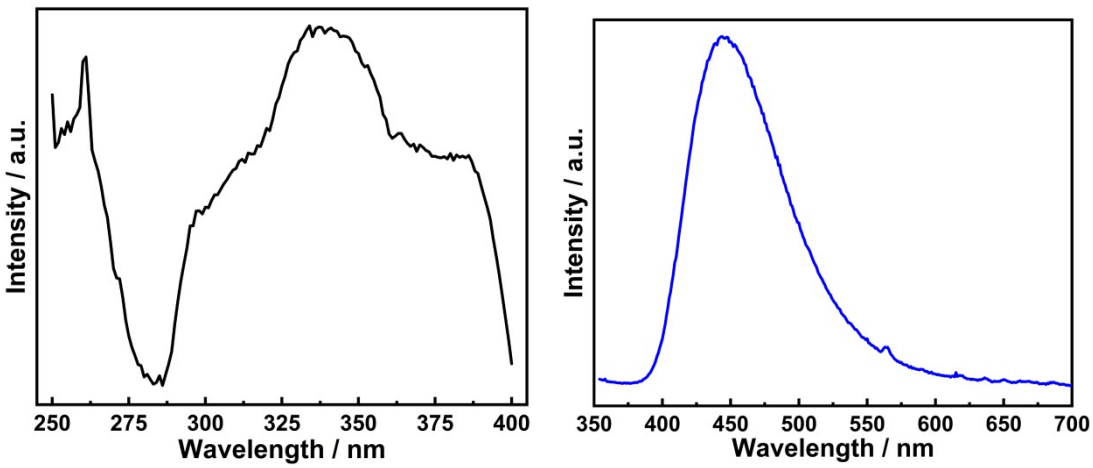

(a) (b)

Fig. S26 Excitation and emission spectra of **6** at 300K.

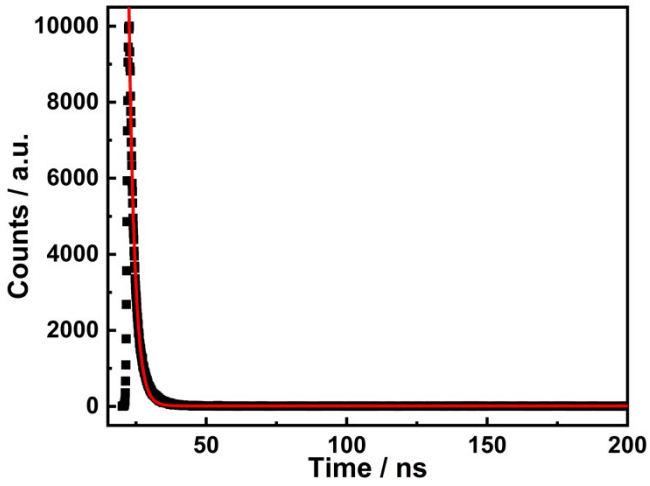

Fig. S27 Lifetime decay curve of **6** at 300K. The red line is the best fit to the single exponential function.

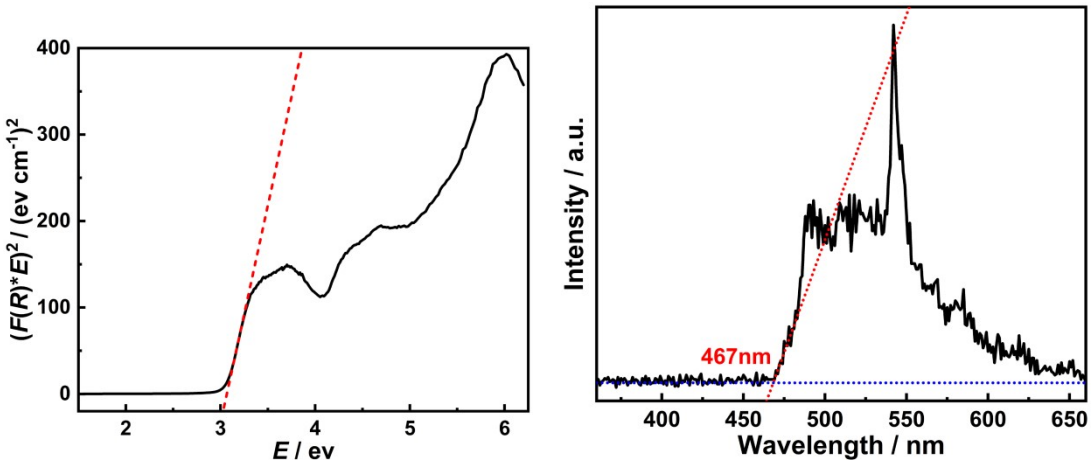

(a) (b)

Fig. S28 (a) Kubelka-Munk Function vs. energy curves of **6**; (b) The phosphorescence spectrum of **6** at 77K.

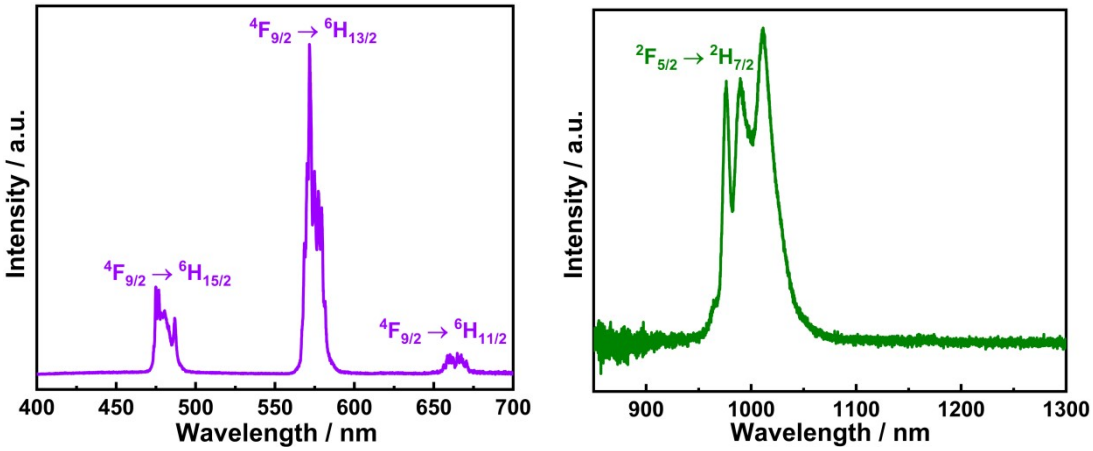

(a) (b)

Fig. S29 The emission spectra of **3** and **5** at 15K.

Table S10. The energy gaps between ground and excited states from luminescence measurements for **3** and **5**.

	3-DyZn /cm^{-1}	**5-YbZn** /cm^{-1}
E0	0	0
E1	40.8	127.6
E2	82.2	200.7
E3	147.4	354.5
E4	247.0	
E5	370.5	

E6	426.1	
E8	516.0	

Synthesis and characterizations of the ligand

Synthesis of the ligand (H_2L , H_2L = 6,6'-dimethoxy-2,2'-[2,2-dimethylpropane -1,3-diylbis- (nitrilomethylidyne)]diphenol)

o-Vanillin (3.04g, 20mmol) was added to a solution of 2,2-dimethyl-1,3-propanediamine (1.02g 10mmol) in EtOH (20mL) and then the mixture was heated at reflux for 2h. After cooling to room temperature, the resulting yellow microcrystal was filtered and was recrystallized using ether to give high quality single crystals. Yield: 2.85g (77%). Calc. (%) for $C_{21}H_{26}N_2O_4$: C 68.09, H 7.07, N 7.56; found: C 68.24, H 7.04, N 7.55. Selected IR data (cm^{-1}): 3321(br), 2902(w), 1638(s), 1529(w), 1475(w), 1373(w), 1256(s), 1227(m), 10798(w), 1052(w), 981(w), 915(w), 780(w), 734(m), 606(w) (Fig. S30).

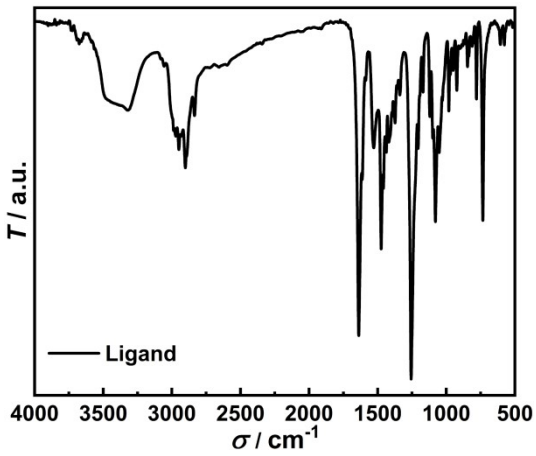

Fig. S30 IR spectra of the ligand.

Single crystal X-ray diffractions reveal that the ligand crystallizes in triclinic space group *P*-1 with *Z* = 4 (Table S1). The asymmetric unit is comprised of two crystallographically independent molecules (Fig. S31). Two imino groups are almost coplanar with the benzene rings. The C=N bond lengths vary from 1.277(2) to 1.304 Å and the relatively short bond length confirms their double bond nature. One phenol group in the molecule is deprotonated and acts as acceptor for the N-H···O hydrogen bond, whereas the other is neutral and acts as donor for the O-H···N hydrogen bond (Fig. S31). These intramolecular hydrogen bonds add stability to the molecules. The molecules are further linked by weak C-H···O/N hydrogen bonds to form a 3D supramolecular framework (Fig. S32). Powder X-ray diffractions show that the experimental PXRD patterns of the ligand are consistent with those extracted from single crystal X-ray diffraction (Fig. S33), confirming its phase purity.

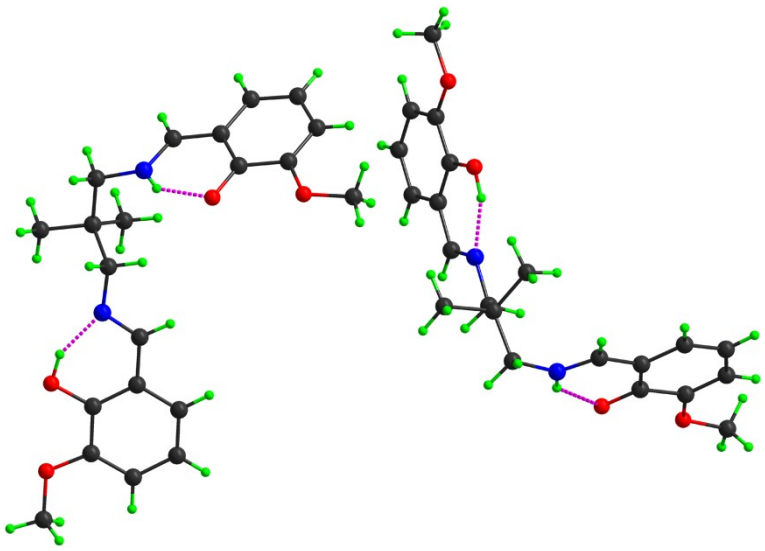

Fig. S31 Molecular structure of the ligand. The pink dash lines represent the intramolecular hydrogen bonds.

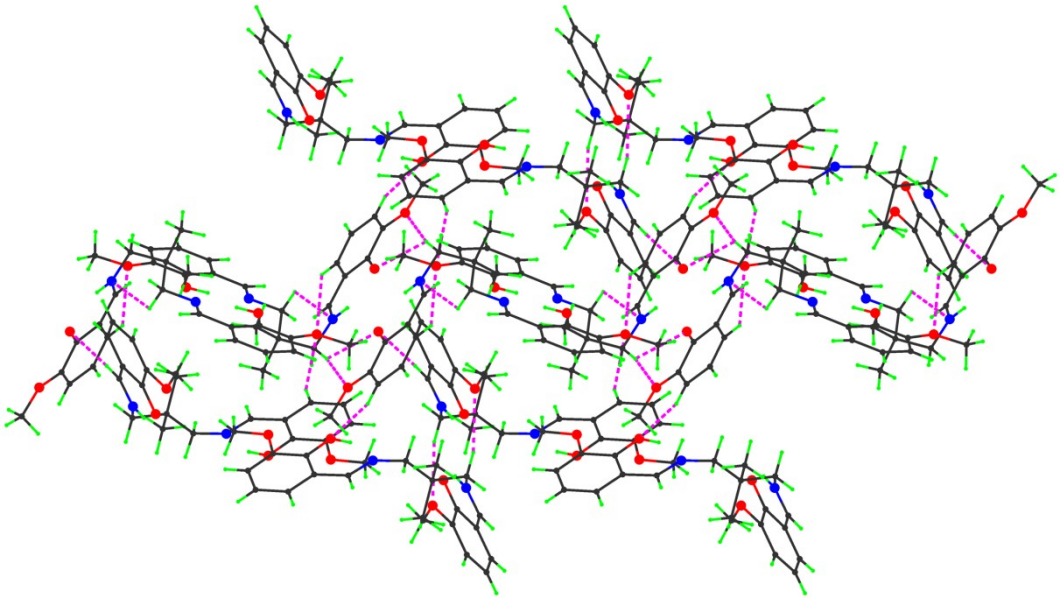

Fig. S32 The 3D supramolecular framework of the ligand. The pink dash lines represent weak intermolecular hydrogen bonds.

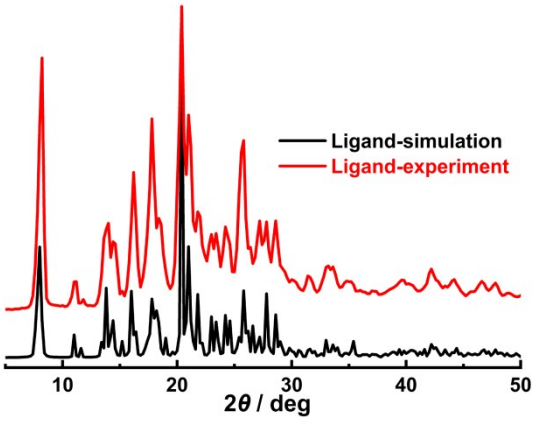

Fig. S33 Measured and simulated PXRD patterns of the ligand.

SQUEEZE results for 1:

SQUEEZE RESULTS (Version = 120716)

Note: Data are Listed for all Voids in the P1 Unit Cell

i.e. Centre of Gravity, Solvent Accessible Volume,

```
# Recovered number of Electrons in the Void and
# Details about the Squeezed Material
loop_
   _platon_squeeze_void_nr
   _platon_squeeze_void_average_x
   _platon_squeeze_void_average_y
   _platon_squeeze_void_average_z
   _platon_squeeze_void_volume
   _platon_squeeze_void_count_electrons
   _platon_squeeze_void_content
    1   0.000   0.000 -0.008        1158          295 ' '
    2   0.500   0.500   0.543        1158          295 ' '
    3   0.000   0.239   0.750           6            0 ' '
    4   0.500   0.261   0.250           6            0 ' '
    5   0.500   0.739   0.750           6            0 ' '
    6   0.000   0.761   0.250           6            0 ' '
# Missing Reflections Below sin(th)/lambda = 0.25
loop_
   _platon_missing_refln_index_h
   _platon_missing_refln_index_k
   _platon_missing_refln_index_l
   _platon_missing_refln_theta
     2     0     0     1.612
     1     1     0     1.442
    -1     1     1     1.485
     1     1     1     2.000
     0     2     1     2.597
    -2     0     2     1.762
     0     0     2     2.024
```

_platon_squeeze_void_probe_radius 1.20

_platon_squeeze_details

'A solvent mask was calculated and 147.5 electrons per molecule were found.

This is consistent with the presence of [NO3],3[C2H3N], 5[H2O] per molecule which account for 148 electrons per molecule.'

SQUEEZE results for 2:

SQUEEZE RESULTS (Version = 120716)

Note: Data are Listed for all Voids in the P1 Unit Cell

i.e. Centre of Gravity, Solvent Accessible Volume,

Recovered number of Electrons in the Void and

Details about the Squeezed Material

loop_

_platon_squeeze_void_nr

_platon_squeeze_void_average_x

_platon_squeeze_void_average_y

_platon_squeeze_void_average_z

_platon_squeeze_void_volume

_platon_squeeze_void_count_electrons

_platon_squeeze_void_content

1 0.000 0.000 -0.007 1164 340 ' '

2 0.500 0.500 0.543 1164 340 ' '

Missing Reflections Below sin(th)/lambda = 0.25

loop_

_platon_missing_refln_index_h

_platon_missing_refln_index_k

_platon_missing_refln_index_l

_platon_missing_refln_theta

2	0	0	1.609
1	1	0	1.442
-1	1	1	1.484
-6	0	2	4.074
-2	0	2	1.753

_platon_squeeze_void_probe_radius 1.20

_platon_squeeze_details

'A solvent mask was calculated and 170 electrons per molecule were found.
This is consistent with the presence of [NO3],4[C2H3N], 5[H2O] per molecule
which account for 170 electrons per molecule.'